Earth and Planetary Science Letters 466 (2017) 12–19

Contents lists available at ScienceDirect

Earth and Planetary Science Letters

www.elsevier.com/locate/epsl

Oxygenation history of the Neoproterozoic to early Phanerozoic and the rise of land plants

Malcolm W. Wallace [a,*], Ashleigh vS. Hood [a,b], Alice Shuster [a], Alan Greig [a], Noah J. Planavsky [b], Christopher P. Reed [a,c]

[a] School of Earth Sciences, University of Melbourne, Parkville, Vic. 3010, Australia
[b] Department of Geology and Geophysics, Yale University, 201 Whitney Ave., New Haven, CT 06511, USA
[c] Teck Resources Chile Ltda., Avenida Isidora Goyenechea N° 2800, Oficina 802, piso 8, Las Condes, Santiago, Chile

ARTICLE INFO

Article history:
Received 1 December 2016
Received in revised form 20 February 2017
Accepted 26 February 2017
Available online xxxx
Editor: M. Frank

Keywords:
ocean oxygenation
carbonate geochemistry
Devonian
plant evolution
rare earth elements
cerium anomaly

ABSTRACT

There has been extensive debate about the history of Earth's oxygenation and the role that land plant evolution played in shaping Earth's ocean–atmosphere system. Here we use the rare earth element patterns in marine carbonates to monitor the structure of the marine redox landscape through the rise and diversification of animals and early land plants. In particular, we use the relative abundance of cerium (Ce_{anom}), the only redox-sensitive rare earth element, in well-preserved marine cements and other marine precipitates to track seawater oxygen levels. Our results indicate that there was only a moderate increase in oceanic oxygenation during the Ediacaran (average Cryogenian $Ce_{anom} = 1.1$, average Ediacaran $Ce_{anom} = 0.62$), followed by a decrease in oxygen levels during the early Cambrian (average Cryogenian $Ce_{anom} = 0.90$), with significant ocean anoxia persisting through the early and mid Paleozoic (average Early Cambrian–Early Devonian $Ce_{anom} = 0.84$). It was not until the Late Devonian that oxygenation levels are comparable to the modern (average of all post-middle Devonian $Ce_{anom} = 0.55$). Therefore, this work confirms growing evidence that the oxygenation of the Earth was neither unidirectional nor a simple two-stage process. Further, we provide evidence that it was not until the Late Devonian, when large land plants and forests first evolved, that oxygen levels reached those comparable to the modern world. This is recorded with the first modern-like negative Ce_{anom} (values <0.6) occurring at around 380 Ma (Frasnian). This suggests that land plants, rather than animals, are the 'engineers' responsible for the modern fully oxygenated Earth system.

1. Introduction

The history of life and surface oxygen levels are inextricably linked (Anbar and Knoll, 2002). Atmospheric oxygen levels are controlled in large part by the extent of organic carbon burial and are thus regulated by the biosphere (Watson et al., 1978). Concurrently, surface oxygen concentrations also play a major role in shaping the structure and composition of the biosphere. For example, the dramatic increase in animal paleobiological diversity and paleoecological complexity recorded at the Neoproterozoic–Phanerozoic transition, arguably one of the most important periods of evolutionary innovation in Earth history, is commonly proposed to have been driven by an oxygenation event (Canfield et al., 2007). Similarly, it has been argued that long-term evolutionary and diversity trends in the Phanerozoic are related to oxygenation (Hannisdal and Peters, 2011). Foremost, vertebrate radiation in the Devonian has been attributed to a marked decrease in the extent of anoxic marine waters (Bambach, 1999; Dahl et al., 2010). An oxygen rise in the Devonian can, in turn, be tied to the rise of the land plants, which likely changed weathering regimes and almost certainly increased the extent of organic matter burial (Algeo and Scheckler, 1998; Lenton et al., 2016). However, much of the discussion of Phanerozoic oxygenation has historically been driven by numerical models, which, for the early Phanerozoic, have large uncertainties and persistent disagreements between varying models (e.g. Bergman et al., 2004; Berner, 2006). Modelling constraints are currently very broad, encompassing a wide range of marine redox conditions which would have had exceedingly disparate impacts upon early animal ecosystems and global biogeochemical cycles. Although several studies have hinted at the possibility of pronounced anoxia during the early Phanerozoic, there are few unambiguous records that provide direct evidence for the proposed Silurian–Devonian oxygen rise (Dahl et al., 2010; Sperling et al., 2015; Lenton et al., 2016).

* Corresponding author. Fax: +61 3 8344 7761.
E-mail address: mww@unimelb.edu.au (M.W. Wallace).

http://dx.doi.org/10.1016/j.epsl.2017.02.046
0012-821X/

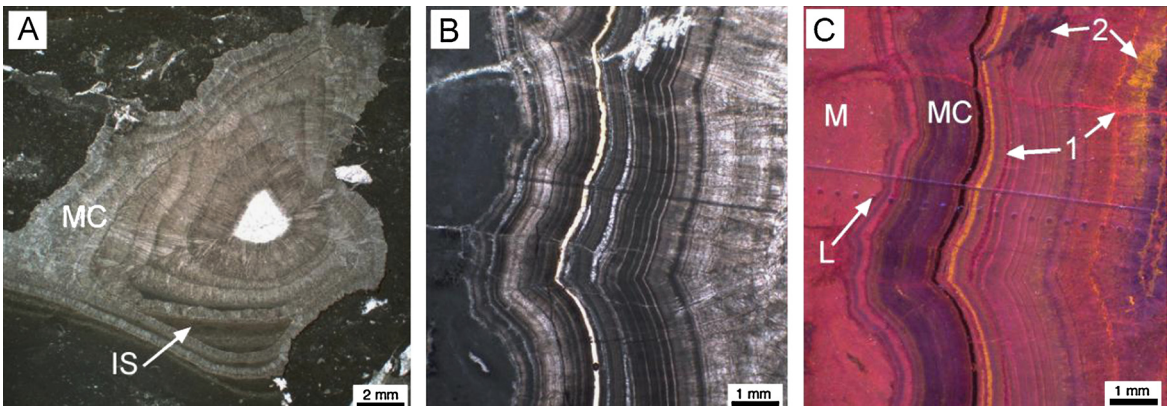

Fig. 1. Examples of well-preserved marine cements. A. Fibrous marine calcite cements (MC) with internal sediments (IS) interlaminated with cements at base of cavity. Upper Devonian Napier Formation, Canning Basin, Western Australia. B. and C. Paired plane light and cathodoluminescence photomicrographs of carbonate microbialite (M) overlain by zoned carbonate marine cements (MC) with laser spots (L) and traverse. Features like cement-filled fractures (1) and areas of irregular luminescence indicating recrystallisation (2) were avoided for analysis. Tonian Devede Formation, Northern Kaokoveld, Namibia.

The chemical behaviour of rare earth elements and yttrium (REEY) are well understood in modern environments and cerium has been widely used as an oceanic paleoredox proxy (Wright et al., 1987; German and Elderfield, 1990; Bau and Dulski, 1996). In particular, several studies (Nothdurft et al., 2004; Webb and Kamber, 2000) indicate that marine microbialites and marine cements may be reliable proxies for the REEY chemistry of ancient oceans. Marine carbonate precipitates can be robust archives for seawater REEY chemistry even through diagenesis and dolomitization (Banner et al., 1988; Nothdurft et al., 2004; Webb et al., 2009), but there can be significant potential for late-stage fluid-rich alteration and/or contamination by clastic sediment. For example, bulk rock analysis of marine carbonates (and other rock types) has serious interpretive problems because of the incorporation of detrital silicates and other non-marine components (like late-stage burial cements and other late diagenetic components) that contaminate the primary marine carbonate REEY signature (Tostevin et al., 2016). Because of the potential for carbonates to include detrital sediment or undergo diagenetic alteration, we have used optical and cathodoluminescence (CL) screening to directly identify well-preserved marine carbonate phases that have not been altered during diagenesis. Specifically, CL work is very useful for distinguishing unaltered primary marine cements, which can be robust archives for paleo-seawater chemistry (Hood and Wallace, 2015).

Therefore, to provide a new perspective on early Phanerozoic surface oxygenation, we have concentrated on the microanalysis of REEY patterns through laser ablation ICP-MS (directly coupled to optical and cathodoluminescence screening) of a suite of shallow-water marine cements and other marine precipitates from a variety of Neoproterozoic and Paleozoic carbonates. This approach has a number of advantages over most previous REEY-based paleoredox studies: 1. Microanalysis (<100 μm spot size) allows diagenetically altered carbonates to be avoided by the application of pre- and post-analysis petrology (Fig. 1); 2. Marine cements are direct precipitates from seawater and contain negligible levels of silicate contamination; 3. Targeted marine cements (e.g. generally fibrous, isopachous and forming macroscopic crusts) are precipitated in high-permeability cavity systems (e.g. reef complexes) that sample unaltered marine fluids; 4. All available constraints suggest these fibrous marine cements are precipitated at a specific depth interval of the ocean (0–400 m) in open-marine conditions.

In our study, REEYs were analysed from eighteen formations (Supplementary Material) ranging in age from Tonian (760 Ma) through to Early Carboniferous (345 Ma) and two Holocene carbonates. All of our analysed samples are from shallow-marine settings, ranging in depth from shallow subtidal through to mid-shelf. Our aim was to use the REEY signature of well-preserved primary marine cements as a guide to the long-term (Neoproterozoic to Paleozoic) oceanic redox state and we have specifically excluded samples from known or suspected short-term anoxic events (e.g. the Late Devonian Frasnian–Famennian boundary). We have also compiled selected published data (Supplementary Material) from twelve other carbonate successions in which there was well documented petrographic screening, six modern seawater surveys and one modern carbonate study in order to produce a more complete record (Fig. 2).

2. Rare earth elements as redox tracers

Rare earth elements are typically present in seawater in their trivalent form and behave similarly to one another. The exception is Ce that has two valence states, the trivalent soluble form and the tetravalent form that is relatively insoluble. Oxidation can therefore preferentially remove Ce relative to the other trivalent rare earths. Removal of Ce is strongly controlled by oxidative scavenging by Mn oxides and hydrous Fe oxides (Bau and Koschinsky, 2009). The presence or absence of Mn and Fe oxides is controlled by the oxidation state of the fluid, providing the link between oxygenation and Ce depletion. Normalisation of Ce abundance relative to the neighbouring rare earths (Ce anomaly or Ce_{anom}) can therefore be used as a measure of oxidative Ce removal. Here we define Ce_{anom} as: $Ce_n/(Pr_n^2/Nd_n)$ (Lawrence et al., 2006), where the subscript n denotes normalisation of concentrations relative to the post-Archean Australian shale (PAAS, McLennan, 1989). This calculation avoids normalisation relative to La, which typically has an over-abundance relative to neighbouring REEs (a La anomaly) in seawater (De Baar et al., 1985). In this calculation, depletion of Ce on normalised REEY profiles (referred to as a negative Ce_{anom} and indicating greater seawater oxygenation) produces values less than 1.0 (1.0 being equivalent to no Ce anomaly).

In modern oxic oceans, a strong negative Ce_{anom} develops in the upper water column (<200 m) and is accentuated at depth with ongoing oxic removal of Ce and concurrent release of other light rare earth elements (LREE) (Alibo and Nozaki, 1999; Moffett, 1994; De Baar et al., 1985; German and Elderfield, 1990). However, in seasonally anoxic or suboxic seawater, the negative Ce_{anom} is not as well developed as it is in well-oxidised seawater (Moffett, 1994). Given that Ce_{anom} in the shallow modern ocean represents a time-averaged record of the redox history of a particular water mass (German and Elderfield, 1990), the proxy tracks basin-scale redox conditions even though anomalies can be controlled by local processes (e.g., local anoxia). Consequently the Ce anomalies

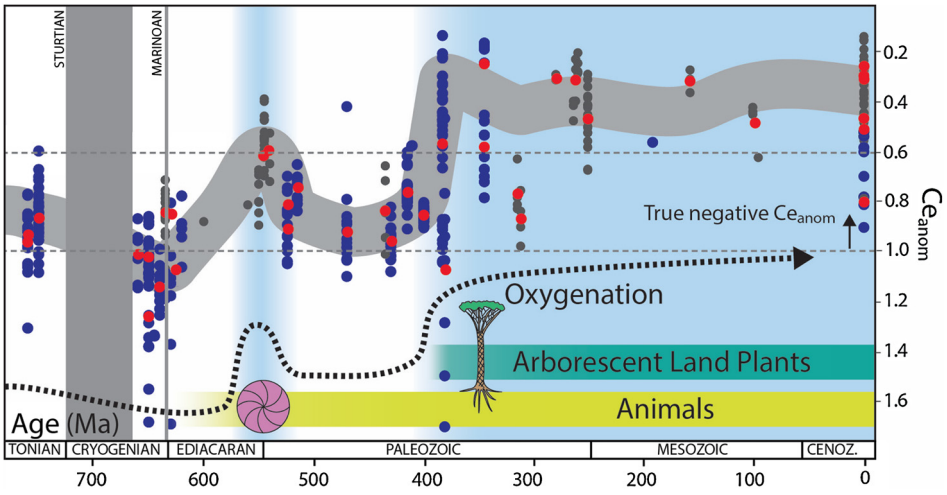

Fig. 2. Plot of the Ce anomaly (Lawrence et al., 2006) from 760 to 0 Ma. Blue circles are analyses from this study. Small grey circles are from published carbonate data (references in Supplementary Material). Red circles are median values for each dataset. Negative Ce anomalies, indicating Ce removal by oxidation, have values less than one. Thick grey line shows the general trend of the Ce anomaly. Dashed black line shows trend of oxygenation. The change to strongly negative Ce anomalies (and a more oxidised ocean) occurs in the Late Devonian, and closely correlates with the evolution of arborescent land plants and forests. Dark grey bars indicate Cryogenian glacial episodes. (For interpretation of the references to colour in this figure legend, the reader is referred to the web version of this article.)

derived from ancient shallow-water carbonates (<400 m depth) are likely to represent an averaged history of the redox chemistry to which that shallow water mass has been exposed. If an ancient ocean basin had an anoxic water body (deep or intermediate waters), then shallow waters would be expected to carry a partial Ce_{anom} signature (i.e. a weaker negative Ce_{anom}) derived from that anoxic water body. For instance, in low atmospheric O_2 conditions, high spatial and temporal variability in shallow marine redox would be expected (Reinhard et al., 2016; Lenton and Daines, 2017), reducing the potential to preserve any negative Ce_{anom} values. Therefore shallow marine carbonates from any environment under oxic conditions with either; intermittent anoxia or exposure to an ocean basin with widespread anoxic deep waters (e.g. a relatively shallow chemocline) would carry only a weakened Ce_{anom} or no Ce_{anom} due to reduced scavenging potential of Ce and variable redox cycling conditions.

Shallow waters, and equivalent marine carbonates only have the possibility to carry a strong negative Ce anomaly in fully oxic marine basins. This, importantly, means that the Ce_{anom} is not entirely a local oxygenation indicator, but is more likely to be derived from an averaged basinal or perhaps global oceanic state. The mean oceanic residence time of Ce is estimated to be around 50–130 yrs (Alibo and Nozaki, 1999) also suggesting that Ce_{anom} is likely to be of basinal or regional origin. Therefore the preservation of a strong negative Ce_{anom} (even with a spread of values towards Ce_{anom} at unity) may be used to mark the occurrence of regionally widespread oxygenated marine conditions at a given time.

The Ce_{anom} value for marine carbonates also appears to be well preserved during carbonate diagenesis, even where diagenesis is intense (Banner et al., 1988; Webb et al., 2009). Webb et al. (2009) found that even during aragonite to calcite conversion in the meteoric environment, the Ce_{anom} value was preserved, but very slightly increased. Virtually all of the marine cements of this study had a primary mineralogy of either calcite or dolomite (particularly in pre-Carboniferous carbonates) and the process of aragonite to calcite conversion would therefore not apply.

3. Methods and materials

In this study, we have used new analytical work (most from marine cements, some from depositional constituents), together with a compilation of published whole rock carbonate and modern oceanic data (details in Supplementary Material). Marine cements were recognised by a number of distinctive characteristics (other than being interlaminated with marine internal sediments), including a fibrous crystallographic texture (radiaxial, radial fibrous or fascicular optic calcite and equivalent fibrous dolomite cements), and an inclusion-rich character. Polished thin sections were examined under plane light and cathodoluminescence microscopy in order to select unaltered primary marine cements for analysis. Cement-filled fractures, stylolites, recrystallised carbonates, non-carbonate inclusions and areas of cross-cutting or irregular luminescence were avoided for analysis. Marine cements were targeted for either uniform non-luminescence (e.g. Phanerozoic samples) or well-preserved CL growth zonation (e.g. Tonian–Cryogenian samples; Fig. 3).

REEY concentrations were determined by LA–ICP–MS on polished, 100–200 µm thick sections. LA–ICP–MS analyses were carried out on a Helex 193 nm ArF excimer laser ablation system connected to an Agilent 7700× quadrupole ICP-MS at the School of Earth Sciences, the University of Melbourne. Operating conditions included a laser repetition rate of 10 Hz and an ablation time of 60 s with spot size ranging from 100 to 150 µm. Blocks of approximately 50 spot analyses on four different samples were analysed at a time with a NIST SRM612 standard analysed every ~7 samples. Data was reduced by Iolite Software (Paton et al., 2011) using the Trace Elements Data Reduction Scheme (Woodhead et al., 2007). Calcium was used as an internal standard element, using the calculated stoichiometric concentrations for either calcite or dolomite (depending on which mineral was being analysed). Outliers were rejected at the ±2 sd level. Limits of detection for the REEYs are typically in the sub-ppb range.

Our new record of Ce_{anom} from the Neoproterozoic to the present day (from 760 to 0 Ma) includes marine cements ($n = 274$) and other marine precipitates ($n = 44$) from this study, in addition to data from previous literature on shallow water marine carbonates (from 115 well documented whole rock, brachiopod, marine cement and coral analyses) and from modern sea water (0–400 m from multiple ocean basins, $n = 28$).

Our compilation of published data is derived from ancient carbonates (12 studies) together with modern seawater and carbonate data (7 studies) (details in Supplementary Material). Most published analyses from ancient carbonates were derived from whole rock data, although some were from marine cements and microbialites. Many of these studies come from reef complexes and platformal carbonates, similar in paleoenvironmental setting to the

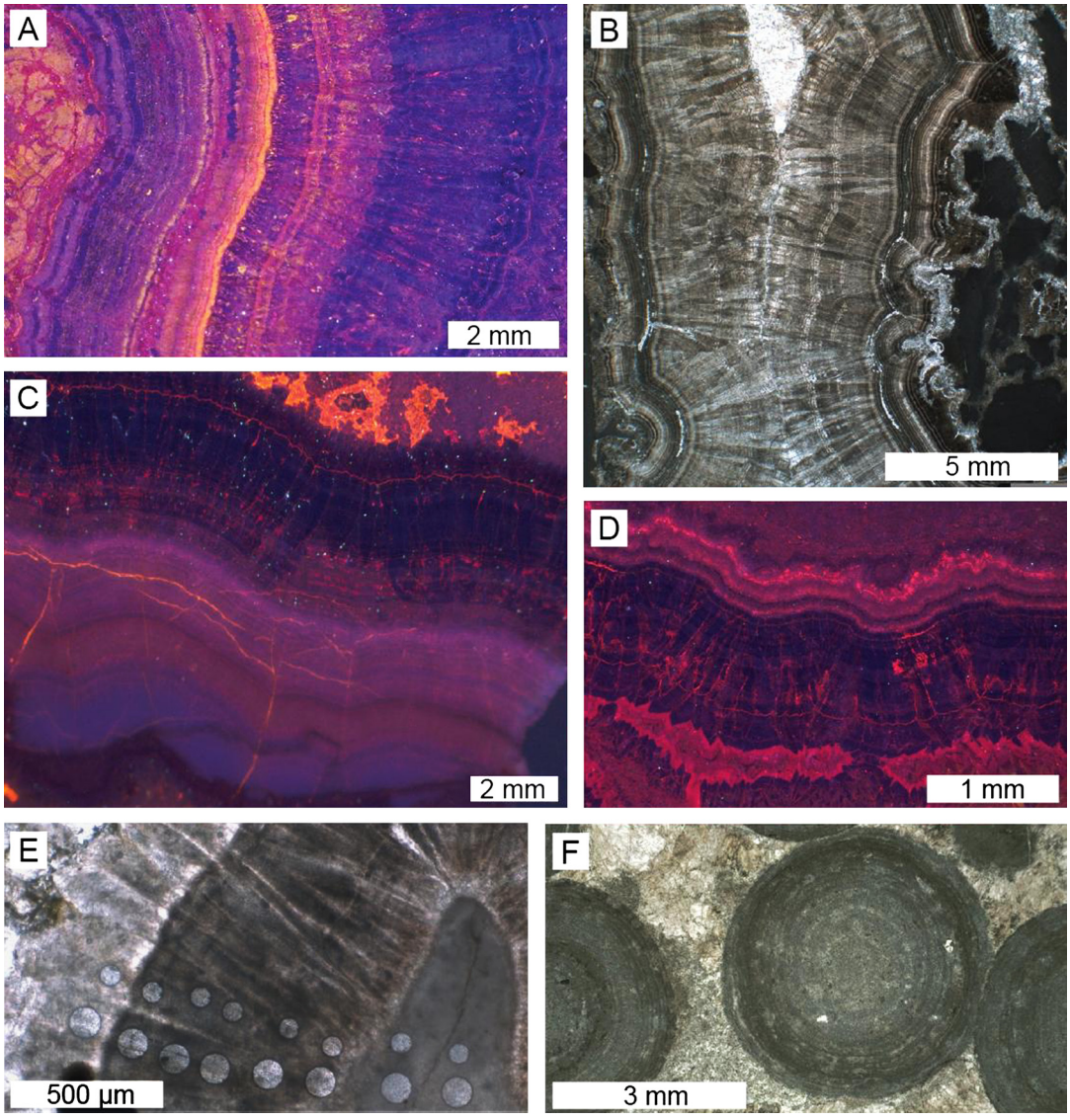

Fig. 3. Cathodoluminescent (CL) and plane light photomicrographs of Tonian samples. A) CL image of marine cements of the Devede Fm., Namibia, sample OKO showing sites of early and late non-luminescent dolomite (dark purple). Laser points avoided late-stage red and yellow veining. B) Plane light image of OKO showing fibrous character. C) CL image of early (diffuse luminescence) and late (non-luminescent) marine cements in the Beck Spring dolomite. Late-stage bright yellow veining was avoided. D) CL image of non-luminescent dolomite fibrous cements in the Beck Spring dolomite, sample SW-1. Late-stage bright red veining was avoided. E) Examples of laser spots form sample EMR-1, Beck Spring Dolomite. F) Sample SS3, showing preserved ooid cortices from Saratoga Springs, Beck Spring Dolomite. (For interpretation of the references to colour in this figure legend, the reader is referred to the web version of this article.)

laser data from this study. To make sure the data was definitively recording marine REEY values in carbonates, studies were only included if the authors considered possible sources of contamination and a sedimentological analysis of what was being analysed. Where authors document contamination of marine values, the analyses were excluded. For example, in data from Jurassic reefs (Olivier and Boyet, 2006), only data from Pagny-sur-Meuse was included because these analyses had the lowest silicate contamination values (as indicated by the authors). Data from the upper Triassic (Ritter et al., 2015) are only taken from samples 1b, 2b, 1t and 2t (Fig. 10 of Ritter et al., 2015) of the earliest marine cements that show no luminescence (Ritter et al., 2015). These data have also been converted from NASC to PAAS normalised. Literature data from modern seawater was selected from a range of seminal papers on the rare earth composition of seawater in the Pacific, Southern and Indian oceans from near-coastal and offshore open ocean waters.

All of the samples from this study (derived or from our analysis) are from pure carbonates, with negligible contamination from clays (e.g. Al vs. Ce_{anom} $r^2 = 0.0021$, median Th = 0.0071 ppm) or oxides (e.g. Fe vs. Ce_{anom} $r^2 = 0.05$). Neither is LREE fractionation (Nd_n/Yb_n) correlated with Ce_{anom} or any detrital element concentrations. Ce_{anom} is instead more strongly correlated with the age of the samples ($r^2 = 0.40$) (Fig. 4).

4. Neoproterozoic–present Ce-anomaly record

Samples that are Cryogenian or Tonian (Fig. 2, 4) have negligible or slightly positive Ce_{anom}, suggesting that these oceans were dominated by waters that were reducing with respect to Ce. Some Cryogenian samples have slightly positive mean Ce_{anom} (mean value 1.10), while Tonian samples have slightly negative Ce_{anom} (mean value 0.89). Early Ediacaran data (from published material of the Doushantuo Formation, and new laser data) have a slightly negative Ce_{anom} (mean value 0.95).

However, mid to late Ediacaran data (from published material of the Dengying and Doushantuo formations) have distinctly negative Ce_{anom} (mean value 0.62), indicating increased removal

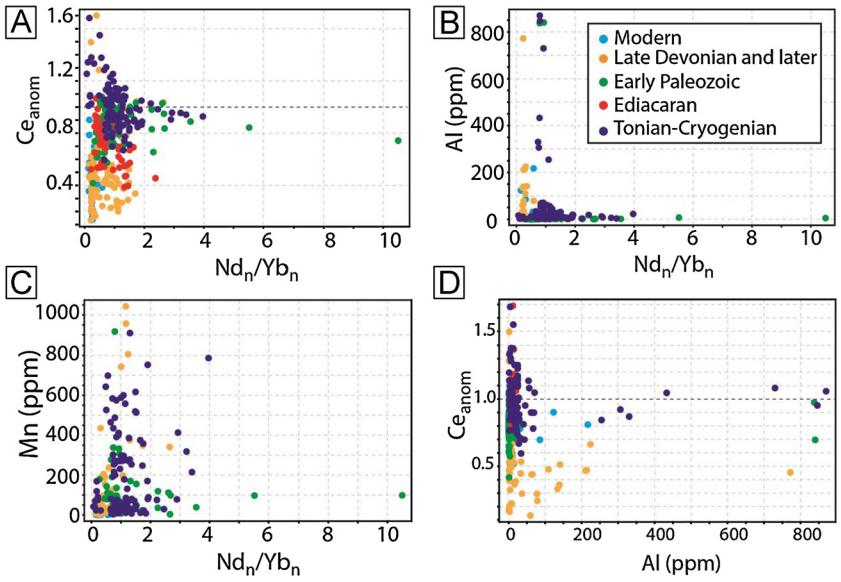

Fig. 4. Contamination and co-variation plots for all data used in the Ce anomaly interpretation. After petrographic screening, samples were screened for Al < 900 ppm and Th < 0.3 ppm and not included if it fell above these levels. These thresholds were chosen based on the point at which REEY profiles were significantly changed (flattened) by REEY derived from clay contamination from the total data set, and are in line with broadly-used cut-off values. A) Ce anomaly does not correlate strongly to LREE depletion (lower Nd_n/Yb_n). B) and C) LREE depletion (Nd_n/Yb_n) does not co-vary with Mn or Al, suggesting neither Mn oxides or clays are contaminating carbonates, or causing normalised profiles to change significantly. D) Ce anomaly does not correlate to Al concentrations, and most samples have less than 50 ppm Al ($\ll$ 1% shale contamination), suggesting clay contamination is not causing a loss of Ce anomaly in samples.

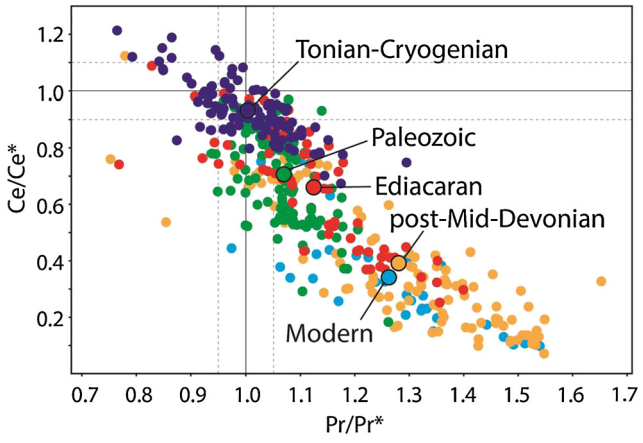

Fig. 5. Conventional Ce vs. Pr anomaly plot binned by time interval (Ce/Ce*, calculated as $= 2Ce_n/(La_n + Nd_n)$ (Bau and Dulski, 1996) vs. Pr anomaly (Pr/Pr* calculated as $= 2Pr_n/(Ce_n + Nd_n)$ (Bau and Dulski, 1996). Mean values for each time bin in black circles. A more pronounced negative Ce anomaly is developed in post-Late Devonian and modern samples. A slight negative Ce anomaly is found in Ediacaran and Paleozoic samples, while earlier Neoproterozoic samples show no Ce anomaly.

of Ce from the water column and increased oxygenation. Following Ediacaran oxygenation, there is a period of weak negative Ce anomalies in the early Paleozoic (Early Cambrian through to Early Devonian mean Ce_{anom} of 0.84), indicating a tendency towards anoxia through this time. The oldest very strong and modern-like negative Ce_{anom} occur in the Late Devonian samples, providing evidence for a strong oceanic oxygenation event during the Devonian. Younger data display strongly negative (but fluctuating) Ce_{anom} to the present day (mean of all post-middle Devonian samples 0.55). Cerium data from shallow modern seawater (0–400 m depth) have similarly strongly negative values (mean Ce_{anom} 0.36).

When binned by time (Tonian–Cryogenian, Ediacaran, Paleozoic, Post-Mid Devonian and modern), shale-normalised REEY data (PAAS, McLennan, 1989) show distinct compositions on conventional Ce vs. Pr anomaly diagrams and distinct profiles on REEY spider diagrams (Figs. 5, 6). Neoproterozoic normalised REEY distributions are slightly enriched in middle rare earth elements (MREEs) and lack a Ce anomaly, whereas Ediacaran profiles are more LREE-depleted, similar to modern seawater. Paleozoic REEY normalised profiles are similar to that of the earlier Neoproterozoic, but have more pronounced Y/Ho and Ce anomalies (Figs. S5, S6). Modern-like REEY profiles are found in post-Mid-Devonian samples and modern carbonates with well-developed negative Ce anomalies and high Y/Ho ratios.

Y/Ho ratios in ancient carbonates have been used as an indicator of marine-like or primary marine chemistry (Nothdurft et al., 2004). This is because Y/Ho ratios are high in seawater relative to those in chondrites (Bau and Koschinsky, 2009). Y/Ho ratios have therefore been used as discriminators of silicate contamination or diagenetic alteration. The Y/Ho ratios of Neoproterozoic carbonates (Fig. S5) are consistently lower than modern marine values, regardless of whether they are whole rock or marine cement analyses. This suggests that the relatively low Y/Ho values of Neoproterozoic carbonates are not the result of silicate contamination and that Y/Ho ratios can be controlled by redox processes (Bau et al., 1997). Y/Ho ratios in marine iron oxides can be lower than chondritic values (Bau and Koschinsky, 2009), suggesting that scavenging by these oxides is what creates superchondritic seawater Y/Ho ratios.

A comparison between post-Mid Devonian data (when the first modern-like Ce_{anom} are seen in the record) and earlier Neoproterozoic to Paleozoic data shows two clearly statistically significant populations (t-test: $p = 2.35 \times 10^{-36}$) (Fig. 7). A Mann–Whitney U test for equal population median values is similarly clearly rejected at the 1% significance level ($p = 1.22 \times 10^{-36}$). Although the data is not normally distributed, bootstrap resampled mean populations show an even clearer distinction between mean Ce_{anom} values before and after the Mid-Devonian, with no overlap in distributions (Fig. 7).

5. Discussion and implications

The consistency of the Ce anomaly (Figs. 2, 5) for time intervals from globally distributed samples suggests that it records global, or at least ocean basin-scale variations in oxygen levels. Early to mid Paleozoic data for example, all show weak negative Ce_{anom} and

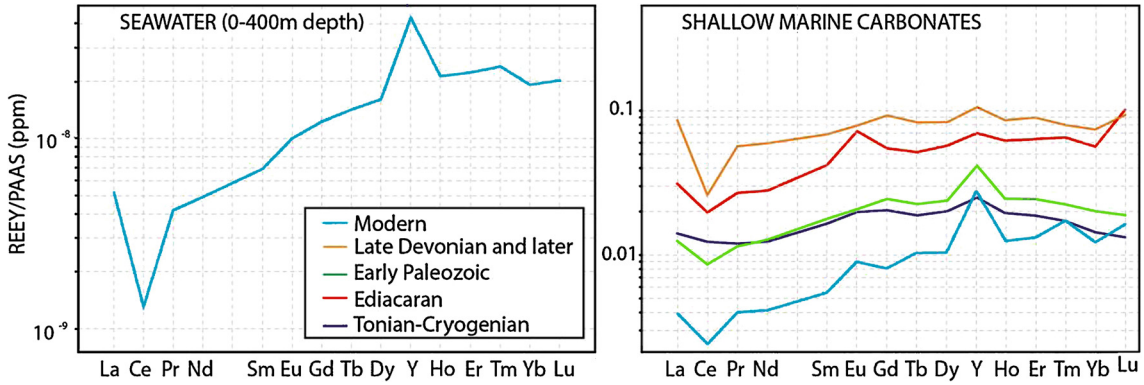

Fig. 6. Average REEY multi-element diagrams from shallow seawater (0–400 m depth) (left) and shallow marine carbonate data (right). Seawater values are taken from the Pacific, Indian, Southern and Atlantic Oceans (Bertram and Elderfield, 1993; De Baar et al., 1985; Nozaki and Alibo, 2003a, 2003b; Shimizu et al., 1994; Zhang and Nozaki, 1996).

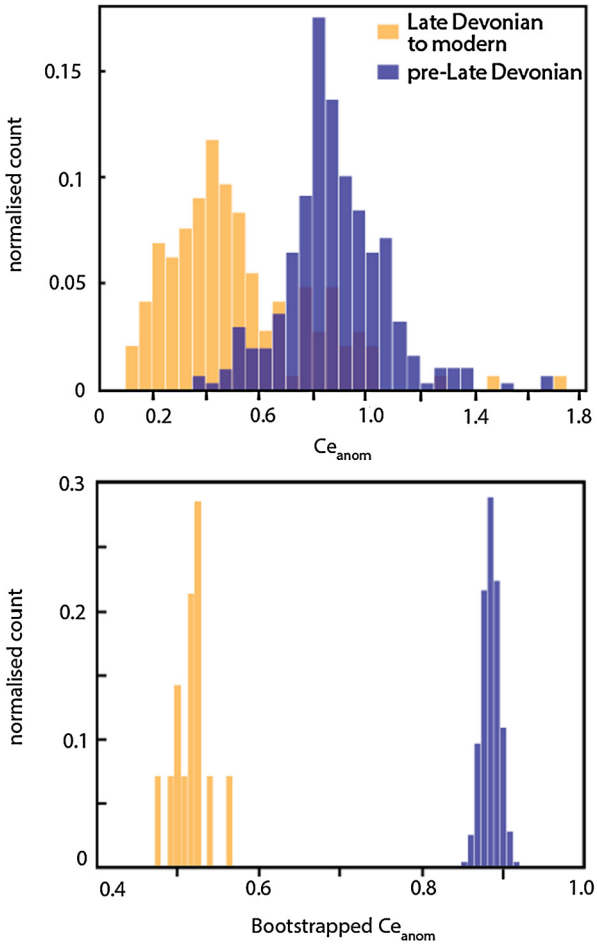

Fig. 7. Distribution of Ce_{anom}. Upper panel: normalised histograms of Ce_{anom} data for all samples (Neoproterozoic–Paleozoic) before the late Devonian (blue) and Late Devonian to modern (yellow) carbonates, including modern seawater values. Lower panel shows bootstrap resampled mean values, with two clearly distinct populations of Ce_{anom} values before and after the Late Devonian. Resampling was completed 10,000 times from each distribution with replacement. (For interpretation of the references to colour in this figure legend, the reader is referred to the web version of this article.)

this is consistent with previously published Mo isotope data (Dahl et al., 2010). The Ce_{anom} data indicate two important episodes of oxygenation in the Neoproterozoic–Phanerozoic (an Ediacaran and a Devonian event) and one episode of de-oxygenation in the Cambrian. The mid to late Ediacaran event coincides with the Neoproterozoic Oxygenation Event, and is consistent with a range of other geochemical paleoredox proxies (Canfield et al., 2007). Moreover, this event correlates with the first appearance and diversification of the Ediacaran fauna (Canfield et al., 2007). However, our data suggest that the Ediacaran event was transient, with a decrease in oxygenation and return to more extensive anoxia during the early to mid Paleozoic (although Ce_{anom} values, and modern-like normalised REEY profiles during this time indicate more oxic overall conditions than in the Tonian–Cryogenian).

The abundance of early Paleozoic graptolitic black shales (Berry and Wilde, 1978), the ratio of organic carbon to pyrite in sediments (Berner and Raiswell, 1983) and shale iron speciation records (Sperling et al., 2015) are consistent with extensive early Paleozoic anoxia. The abundance of Paleozoic black shales was recognised by early workers like Ruedemann (1935) who listed black shales from the New York region ranging in age from Cambrian through to Mid Devonian.

The episode of oxygenation in the Devonian has not been well documented geochemically. There is potentially Mo isotope evidence for a Devonian oxygenation event (Dahl et al., 2010; Lenton et al., 2016). Our Ce_{anom} dataset is in broad agreement with the sparse Mo isotope record, but the Ce_{anom} data provides a clearer geochemical record of both the Ediacaran and Devonian events. The very strong negative Ce_{anom} in Late Devonian and early Carboniferous samples closely correlates with the diversification of land plants during this period (Algeo and Scheckler, 1998). While spore records suggest terrestrial floras had evolved by the middle Ordovician, these early land plants were small and non-vascular (Algeo and Scheckler, 1998).

It has been suggested that these small mid-Paleozoic plants played a significant role in modifying terrestrial ecosystems and global weathering prior to the Late Devonian (Lenton et al., 2016; Porada et al., 2016), although other researchers suggest that these early "cryptogamic" plants were probably not significant in this respect (Edwards et al., 2015). Our Ce_{anom} record shows a slight rise in the cerium anomaly beginning in the Early Devonian and this may correspond with the spread of very early vascular plants (Lenton et al., 2016). However, our Ce_{anom} record does not increase to levels comparable with that of the modern cerium anomaly until the Late Devonian (Frasnian) (Fig. 2). This increase closely coincides with the evolution of large arborescent vascular plants, first recorded in the Mid-Devonian (Givetian, Stein et al., 2007) and this may suggest that the evolution of trees and forests played a significant role in influencing the carbon cycle and atmospheric oxygen levels (Edwards et al., 2015).

The Paleozoic charcoal record also offers insights into the evolution of plants and atmospheric oxygen during this time (Lenton et al., 2016). The first appearance of charcoal in the Late Silurian (Glasspool et al., 2004) and its low abundance through the Devo-

nian have been used to indicate O_2 concentrations greater than 15–17% through this period (Belcher and McElwain, 2008). This charcoal data potentially supports the hypothesis of an increase in oxygenation beginning earlier than the Devonian (Lenton et al., 2016). Significantly, the charcoal record also shows an enormous increase in abundance (1–2 orders of magnitude) in the Late Devonian (Lenton et al., 2016), consistent with our Ce_{anom} record and consistent with large arborescent plants playing an important role in oxygenation.

The evolution of vascular plants began in the Late Silurian and by the Late Devonian, all of the major plant groups had evolved arborescent species (Algeo and Scheckler, 1998). Forests driving oxygenation should not be a surprise, as trees produce recalcitrant organic matter with C/P ratios that are much higher than marine primary producers (Kump, 1988). The preservation and burial of abundant terrestrial organic material during late Paleozoic time was a giant new source of oxygen production (Algeo and Scheckler, 1998; Algeo and Ingall, 2007). The evolution and increased abundance of a terrestrial biomass more resistant to bacterial breakdown (lignin-rich material, Robinson, 1990) in the Late Devonian meant that transported organic matter was more likely to be preserved in a marine setting, (even with co-evolution of lignin-degrading fungi, Nelsen et al., 2016) also contributing to oxygenation (Kump, 1988). Therefore the Ce_{anom} data compiled here provides strong empirical evidence linking ocean oxygenation and the evolution of large, vascular land plants.

6. Conclusions

The typical narrative is that Earth became oxidised in two major steps (the Great Oxygenation Event and the Neoproterozoic Oxygenation Event) that neatly subdivide earth history into three stages; Archean, Proterozoic and Phanerozoic, each stage being more oxic than the last. However, our results suggest this simple picture of Earth's oxygenation history is incorrect and reality, not unexpectedly, is considerably more complex. It now appears more likely that there was a protracted and irregular Oxygenation increase that extended well into the Phanerozoic. This suggests that the Neoproterozoic Oxygenation Event was only a small step towards a modern oxygenated Earth system. The rise of land plants appears to have been essential for the permanent transition to fully oxygenated oceans.

Author contributions

M.W.W and A.vS.H conceived the project, A.vS.H compiled the data, M.W.W, A.vS.H, C.P.R. and A.S. collected samples, A.vS.H, A.S., M.W.W and A.G. carried out analyses, M.W.W and A.vS.H wrote the paper, with input from all co-authors.

Author information

The authors declare no competing financial interests.

Acknowledgements

This research was partially funded from ARC Discovery Grant DP130102240 to MWW. AvSH acknowledges funding from a NAI Postdoctoral Fellowship. NJP acknowledges funding from NSF-ELT program and the Alternative Earths NASA Astrobiology Institute. We are grateful to Doug and Marg Sprigg for field support over many years. Teck Ltd provided field support and access to drill core in Namibia and Ireland. Reviews by Thomas Algeo, Tim Lenton and Balz Kamber significantly improved the manuscript and we thank the reviewers for their contribution.

Appendix A. Supplementary material

Supplementary material related to this article can be found online at http://dx.doi.org/10.1016/j.epsl.2017.02.046.

References

Algeo, T.J., Ingall, E., 2007. Sedimentary C_{org}:P ratios, paleocean ventilation, and Phanerozoic atmospheric pO_2. Palaeogeogr. Palaeoclimatol. Palaeoecol. 256, 130–155.

Algeo, T.J., Scheckler, S.E., 1998. Terrestrial-marine teleconnections in the Devonian: links between the evolution of land plants, weathering processes, and marine anoxic events. Philos. Trans. R. Soc. Lond. B, Biol. Sci. 353, 113–130.

Alibo, D.S., Nozaki, Y., 1999. Rare earth elements in seawater: particle association, shale-normalization, and Ce oxidation. Geochim. Cosmochim. Acta 63, 363–372.

Anbar, A.D., Knoll, A., 2002. Proterozoic ocean chemistry and evolution: a bioinorganic bridge? Science 297, 1137–1142.

Bambach, R.K., 1999. Energetics in the global marinefauna: a connection between terrestrial diversification and change in the marine biosphere. Geobios 32, 131–144.

Banner, J.L., Hanson, G., Meyers, W., 1988. Rare earth element and Nd isotopic variations in regionally extensive dolomites from the Burlington–Keokuk Formation (Mississippian): implications for REE mobility during carbonate diagenesis. J. Sediment. Res. 58, 415–432.

Bau, M., Dulski, P., 1996. Distribution of yttrium and rare-earth elements in the Penge and Kuruman iron-formations, Transvaal Supergroup, South Africa. Precambrian Res. 79, 37–55.

Bau, M., Koschinsky, A., 2009. Oxidative scavenging of cerium on hydrous Fe oxide: evidence from the distribution of rare earth elements and yttrium between Fe oxides and Mn oxides in hydrogenetic ferromanganese crusts. Geochem. J. 43, 37–47.

Bau, M., Möller, P., Dulski, P., 1997. Yttrium and lanthanides in eastern Mediterranean seawater and their fractionation during redox-cycling. Mar. Chem. 56, 123–131.

Belcher, C.M., McElwain, J.C., 2008. Limits for combustion in low O_2 redefine paleoatmospheric predictions for the Mesozoic. Science 321, 1197–1200.

Bergman, N.M., Lenton, T.M., Watson, A.J., 2004. COPSE: a new model of biogeochemical cycling over Phanerozoic time. Am. J. Sci. 304, 397–437.

Berner, R.A., 2006. GEOCARBSULF: a combined model for Phanerozoic atmospheric O_2 and CO_2. Geochim. Cosmochim. Acta 70, 5653–5664.

Berner, R.A., Raiswell, R., 1983. Burial of organic carbon and pyrite sulfur in sediments over Phanerozoic time: a new theory. Geochim. Cosmochim. Acta 47, 855–862.

Berry, W.B., Wilde, P., 1978. Progressive ventilation of the oceans; an explanation for the distribution of the lower Paleozoic black shales. Am. J. Sci. 278, 257–275.

Bertram, C.J., Elderfield, H., 1993. The geochemical balance of the rare earth elements and neodymium isotopes in the oceans. Geochim. Cosmochim. Acta 57, 1957–1986.

Canfield, D.E., Poulton, S.W., Narbonne, G.M., 2007. Late-Neoproterozoic deep-ocean oxygenation and the rise of animal life. Science 315, 92–95.

Dahl, T.W., Hammarlund, E.U., Anbar, A.D., Bond, D.P., Gill, B.C., Gordon, G.W., Knoll, A.H., Nielsen, A.T., Schovsbo, N.H., Canfield, D.E., 2010. Devonian rise in atmospheric oxygen correlated to the radiations of terrestrial plants and large predatory fish. Proc. Natl. Acad. Sci. USA 107, 17911–17915.

De Baar, H.J., Bacon, M.P., Brewer, P.G., Bruland, K.W., 1985. Rare earth elements in the Pacific and Atlantic Oceans. Geochim. Cosmochim. Acta 49, 1943–1959.

Edwards, D., Cherns, L., Raven, J.A., 2015. Could land-based early photosynthesizing ecosystems have bioengineered the planet in mid-Palaeozoic times? Palaeontology 58, 803–837.

German, C.R., Elderfield, H., 1990. Application of the Ce anomaly as a paleoredox indicator: the ground rules. Paleoceanography 5, 823–833.

Glasspool, I.J., Edwards, D., Axe, L., 2004. Charcoal in the Silurian as evidence for the earliest wildfire. Geology 32, 381–383.

Hannisdal, B., Peters, S.E., 2011. Phanerozoic Earth system evolution and marine biodiversity. Science 334, 1121–1124.

Hood, A.vS., Wallace, M.W., 2015. Extreme ocean anoxia during the Late Cryogenian recorded in reefal carbonates of Southern Australia. Precambrian Res. 261, 96–111.

Kump, L.R., 1988. Terrestrial feedback in atmospheric oxygen regulation by fire and phosphorus. Nature 335, 152–154.

Lawrence, M.G., Greig, A., Collerson, K.D., Kamber, B.S., 2006. Rare earth element and yttrium variability in South East Queensland waterways. Aquat. Geochem. 12, 39–72.

Lenton, T.M., Dahl, T.W., Daines, S.J., Mills, B.J., Ozaki, K., Saltzman, M.R., Porada, P., 2016. Earliest land plants created modern levels of atmospheric oxygen. Proc. Natl. Acad. Sci. USA, 9704–9709.

Lenton, T.M., Daines, S.J., 2017. Biogeochemical transformations in the history of the ocean. Annu. Rev. Mar. Sci. 9, 31–58.

McLennan, S., 1989. Rare earth elements in sedimentary rocks; influence of provenance and sedimentary processes. In: Lipin, B.R., McKay, G.A. (Eds.), Geochemistry and Mineralogy of Rare Earth Elements. In: Rev. Miner., vol. 21. Mineralogical Society of America, pp. 169–200.

Moffett, J.W., 1994. A radiotracer study of cerium and manganese uptake onto suspended particles in Chesapeake Bay. Geochim. Cosmochim. Acta 58, 695–703.

Nelsen, M.P., DiMichele, W.A., Peters, S.E., Boyce, C.K., 2016. Delayed fungal evolution did not cause the Paleozoic peak in coal production. Proc. Natl. Acad. Sci. USA 113, 2442–2447.

Nothdurft, L.D., Webb, G.E., Kamber, B.S., 2004. Rare earth element geochemistry of Late Devonian reefal carbonates, Canning Basin, Western Australia: confirmation of a seawater REE proxy in ancient limestones. Geochim. Cosmochim. Acta 68, 263–283.

Nozaki, Y., Alibo, D.S., 2003a. Dissolved rare earth elements in the Southern Ocean, southwest of Australia: unique patterns compared to the South Atlantic data. Geochem. J. 37, 47–62.

Nozaki, Y., Alibo, D.S., 2003b. Importance of vertical geochemical processes in controlling the oceanic profiles of dissolved rare earth elements in the northeastern Indian Ocean. Earth Planet. Sci. Lett. 205, 155–172.

Olivier, N., Boyet, M., 2006. Rare earth and trace elements of microbialites in Upper Jurassic coral- and sponge-microbialite reefs. Chem. Geol. 230, 105–123.

Paton, C., Hellstrom, J., Paul, B., Woodhead, J., Hergt, J., 2011. Iolite: freeware for the visualisation and processing of mass spectrometric data. J. Anal. At. Spectrom. 26, 2508–2518.

Porada, P., Lenton, T.M., Pohl, A., Weber, B., Mander, L., Donnadieu, Y., Beer, C., Pöschl, U., Kleidon, A., 2016. High potential for weathering and climate effects of non-vascular vegetation in the Late Ordovician. Nat. Commun. 7, 12113. http://dx.doi.org/10.1038/ncomms12113.

Reinhard, C.T., Planavsky, N.J., Olson, S.L., Lyons, T.W., Erwin, D.H., 2016. Earth's oxygen cycle and the evolution of animal life. Proc. Natl. Acad. Sci. USA 113, 8933–8938.

Ritter, A.-C., Kluge, T., Berndt, J., Richter, D.K., John, C.M., Bodin, S., Immenhauser, A., 2015. Application of redox sensitive proxies and carbonate clumped isotopes to Mesozoic and Palaeozoic radiaxial fibrous calcite cements. Chem. Geol. 417, 306–321.

Robinson, J.M., 1990. Lignin, land plants, and fungi: biological evolution affecting Phanerozoic oxygen balance. Geology 18, 607–610.

Ruedemann, R., 1935. Ecology of black mud shales of Eastern New York. J. Paleontol. 9, 79–91.

Shimizu, H., Tachikawa, K., Masuda, A., Nozaki, Y., 1994. Cerium and neodymium isotope ratios and REE patterns in seawater from the North Pacific Ocean. Geochim. Cosmochim. Acta 58, 323–333.

Sperling, E.A., Wolock, C.J., Morgan, A.S., Gill, B.C., Kunzmann, M., Halverson, G.P., Macdonald, F.A., Knoll, A.H., Johnston, D.T., 2015. Statistical analysis of iron geochemical data suggests limited Late Proterozoic oxygenation. Nature 523, 451–454.

Stein, W.E., Mannolini, F., Hernick, L.V., Landing, E., Berry, C.M., 2007. Giant cladoxylopsid trees resolve the enigma of the Earth's earliest forest stumps at Gilboa. Nature 446, 904–907.

Tostevin, R., Shields, G.A., Tarbuck, G.M., He, T., Clarkson, M.O., Wood, R.A., 2016. Effective use of cerium anomalies as a redox proxy in carbonate-dominated marine settings. Chem. Geol. 438, 146–162.

Watson, A., Lovelock, J.E., Margulis, L., 1978. Methanogenesis, fires and the regulation of atmospheric oxygen. Biosystems 10, 293–298.

Webb, G.E., Kamber, B.S., 2000. Rare earth elements in Holocene reefal microbialites: a new shallow seawater proxy. Geochim. Cosmochim. Acta 64, 1557–1565.

Webb, G.E., Nothdurft, L.D., Kamber, B.S., Kloprogge, J., Zhao, J.X., 2009. Rare earth element geochemistry of scleractinian coral skeleton during meteoric diagenesis: a sequence through neomorphism of aragonite to calcite. Sedimentology 56, 1433–1463.

Woodhead, J.D., Hellstrom, J., Hergt, J.M., Greig, A., Maas, R., 2007. Isotopic and elemental imaging of geological materials by laser ablation inductively coupled plasma-mass spectrometry. Geostand. Geoanal. Res. 31, 331–343.

Wright, J., Schrader, H., Holser, W.T., 1987. Paleoredox variations in ancient oceans recorded by rare earth elements in fossil apatite. Geochim. Cosmochim. Acta 51, 631–644.

Zhang, J., Nozaki, Y., 1996. Rare earth elements and yttrium in seawater: ICP-MS determinations in the East Caroline, Coral Sea, and South Fiji basins of the western South Pacific Ocean. Geochim. Cosmochim. Acta 60, 4631–4644.